JOC The Journal of Organic Chemistry

Article

pubs.acs.org/joc

Mechanistic Insights into the Cu(I)- and Cu(II)-Catalyzed Cyclization of *o*-Alkynylbenzaldehydes: The Solvent DMF and Oxidation State of Copper Affect the Reaction Mechanism

Binfang Yuan, Rongxing He, Wei Shen, Cheng Huang, and Ming Li*

Key Laboratory of Luminescence and Real-Time Analytical chemistry (Southwest University), Ministry of Education, College of Chemistry and Chemical Engineering, Southwest University, Chongqing 400715, China

Supporting Information

ABSTRACT: A computational study with the BhandHLYP density functional is conducted to elucidate the mechanisms of Cu(I)- and Cu(II)-catalyzed reactions of *o*-alkynylbenzaldehydes with a nucleophile (MeOH). Our calculations suggest the following. (a) The use of CuCl as a catalyst deceases significantly the energy barrier and promotes intramolecular cyclization. (b) Solvent DMF is critical in the stepwise hydrogen-transport process involved in an intermolecular nucleophilic addition because it can greatly reduce the free energy barrier of the hydrogen-transfer process as a proton shuttle. In addition, we find that substrate MeOH also plays a role similar to that of DMF in the hydrogen-transport reaction. (c) The 6-endo product P1 is formed exclusively using a catalytic system consisting of CuCl and DMF, whereas a mixture of 6-endo product P1 and 5-exo product P2 in a ratio of ~1:1 is produced using $CuCl_2$ and DMF as a catalytic system. Our theoretical calculations reproduce the experimental results very well. This study is expected to improve our understanding of Cu(I)- and Cu(II)-catalyzed reactions involving Lewis base solvents and to provide guidance for the future design of new catalysts and new reactions.

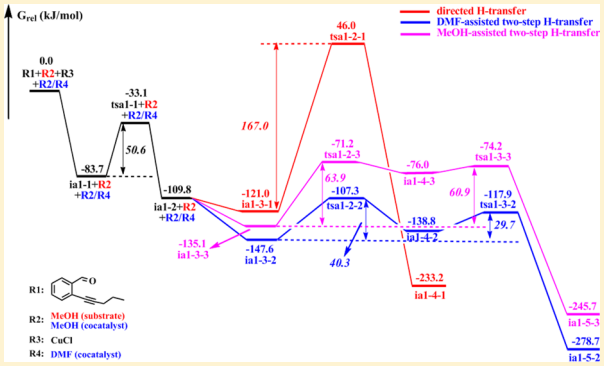

1. INTRODUCTION

It is well-known that solvents play an important role in organic synthesis reactions.[1] A large number of experimental and theoretical studies have been conducted to supplement the information concerning the influence of solvents on chemical and biological reactions.[2] As reaction media, solvents can generally affect yields of reactions or even change reaction mechanisms.[3] Furthermore, satisfactory results can also be obtained when solvents participate directly in reactions.[4] In a word, the solvents in many reactions play a critical role in producing rate acceleration and higher selectivity.

A significant function of solvents is to improve the yield of catalytic reactions. Lee et al.[5] discovered that DMF is the best solvent among several that were examined (DMF, THF, and CH_3CN), which leads to the formation of (*E*)-*α*-ethynyl-*α*,*β*-unsaturated esters in excellent yields under mild conditions. A similar phenomenon was also reported by Ma and Lei et al.[6] In addition, combination of two solvents could also yield good results.[7] For example, Wu and co-workers[8] found that the combination of dichloroethane (DCE) and CCl_4 acts as a favorable catalytic medium to give the best yields in the AgOTf-catalyzed tandem reaction of *N*′-(2-alkynylbenzylidene)-hydrazide with alkynes. Besides, solvent and metal catalyst can be combined into a new catalytic system to promote the Cu(I)-catalyzed synthesis of furans from 2-(1-alkynyl)-2-alken-1-ones in DMF.[9] This fact was supported by the work of Pal, Fujimoto, and Huang et al.[10] Another significant function of solvents is to control reaction selectivity, which has aroused a great deal of attention of many researchers. Doyle and co-workers[11] reported that the 1,3-dipolar cycloaddition of nitrones with *α*,*β*-unsaturated aldehydes catalyzed by a cationic chiral dirhodium (II, III) carboxamidate has a high selectivity when toluene is used as solvent. A similar situation was also observed by Wang et al.[12] in the Au-catalyzed reaction of propargylic sulfides and dithioacetals. Gevorgyan et al.[13] found that in the Au(III)-catalyzed regiodivergent synthesis of halofurans, the selectivity of the reaction can be changed with solvent polarity. In short, the results described above indicate that solvent has a great influence on the yield and selectivity of reactions. However, the detailed mechanisms of chemical reactions affected by solvents have not been illustrated clearly to date, which should be studied further.

At the same time, the use of transition metals as catalysts has attracted more attention in modern organic chemistry.[14] In general, there are two important kinds of functions for those catalysts in organic synthesis reactions. First, the reaction can be conducted smoothly in the presence of transition metal catalysts. For example, the intramolecular o-vinylation of carbonyl compounds can be preceded favorably using CuI as

Received: March 8, 2015
Published: June 2, 2015

DOI: 10.1021/acs.joc.5b00523
J. Org. Chem. 2015, 80, 6553−6563

Scheme 1. Baldwin's Rules[19] Apply to the Cu(I)- and Cu(II)-Catalyzed Reactions of *o*-Alkynylbenzaldehydes with MeOH

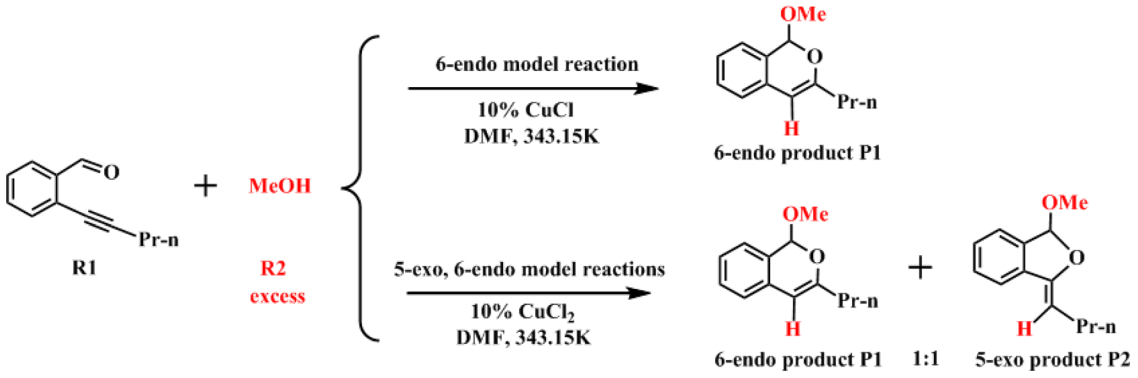

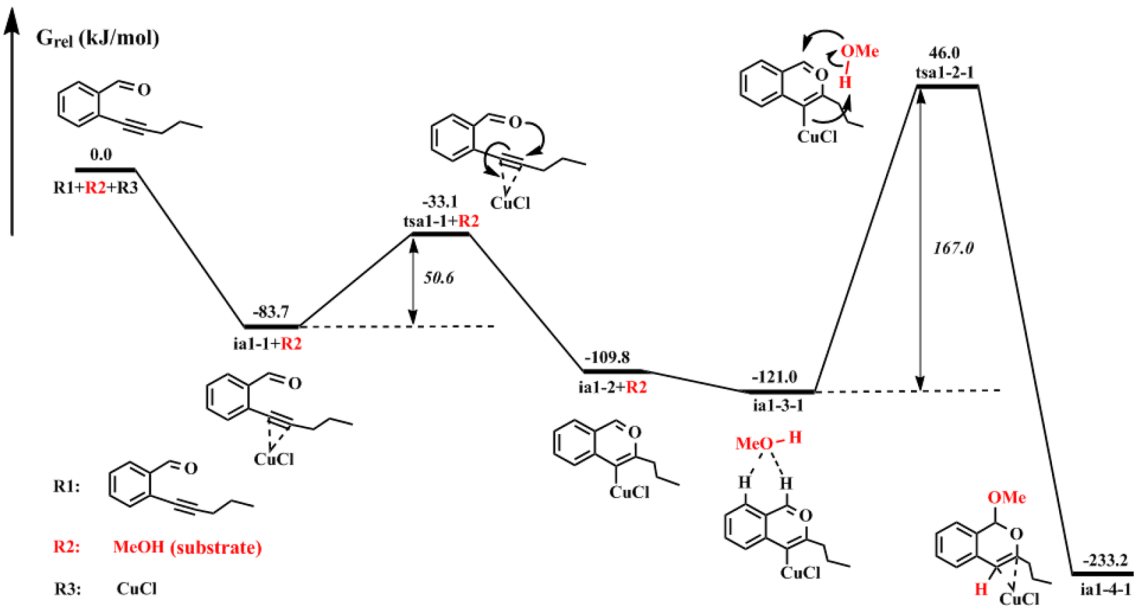

Figure 1. DFT-computed energy profile for the Cu(I)-catalyzed 6-endo model reaction without a cocatalyst in DMF medium.

a catalyst, while no reaction occurs in the absence of copper catalysts; this experimental result was found by Li et al.[15] Second, the transition metal catalysts can control the selectivity of reactions.[13,16] The metallic valence state of transition metal catalysts is a key factor for the selective control of organic synthesis reactions.[17] However, the influence of the metallic valence state on the selectivity of organic synthesis is important, but not clear. On the basis of the reasons mentioned above, exploration of the effects of the transition metal catalysts on the catalytic reaction, especially for the selectivity of reaction, is very critical.

To further understand the roles of solvents and transition metal catalysts in organic reaction, the Cu(I)- and Cu(II)-catalyzed synthesis of cyclic alkenyl ethers form *o*-alkynylbenzaldehydes (R1) and MeOH (R2) in DMF medium[18] (as shown in Scheme 1) is selected as a simple template to better explore the following issues in detail: (a) the role of the metal catalyst in the reaction, (b) how solvent DMF promotes the reaction and whether excess MeOH (one of the reactants) plays a role similar to that of DMF, and (c) how the metallic valence state of copper controls the selectivity of the reaction.

2. COMPUTATIONAL METHODS

All calculations are conducted with the Gaussian 09 programs.[20] The geometries of all the intermediates and transition states are fully optimized by using the BhandHLYP method of density functional theory (DFT),[21] which is based on the Becke's half-and-half method[22] and the gradient-corrected correlation functional of Lee and co-workers.[23] The DFT method has been proven to be reliable in numerous theoretical simulations of mechanisms of metal-catalyzed reactions.[24] For geometric optimizations, the 6-31G* basis set[25] is used for Cl, C, O, and H elements; Cu is described by the LanL2DZ[26] basis set. When $CuCl_2$ is selected as a catalyst to replace CuCl, the spin state of Cu is set to $s = 2$ ($s = 1$ in CuCl). Frequency calculations at the same level of theory are used to characterize all of the stationary points (no imaginary frequency for an equilibrium structure and one imaginary frequency for a transition state structure). In several cases where transition states are not easily confirmed by animation of their vibrations, intrinsic reaction coordinate (IRC)[27] calculations are performed to unambiguously connect the transition states with the reactants and the products (all IRC calculations are collected in the Supporting Information). The charge decomposition analysis (CDA) and the construction of orbital interaction diagrams are performed using AOMix-CDA code.[28] The effects of solvent on energies are calculated on the basis of the gas phase-optimized structures with the polarized continuum model (PCM).[29] The dielectric constant in the PCM computations is set to $\varepsilon = 37.22$ to simulate DMF. The single-point energies are also computed using the PCM/BhandHLYP/6-

DOI: 10.1021/acs.joc.5b00523
J. Org. Chem. 2015, 80, 6553−6563

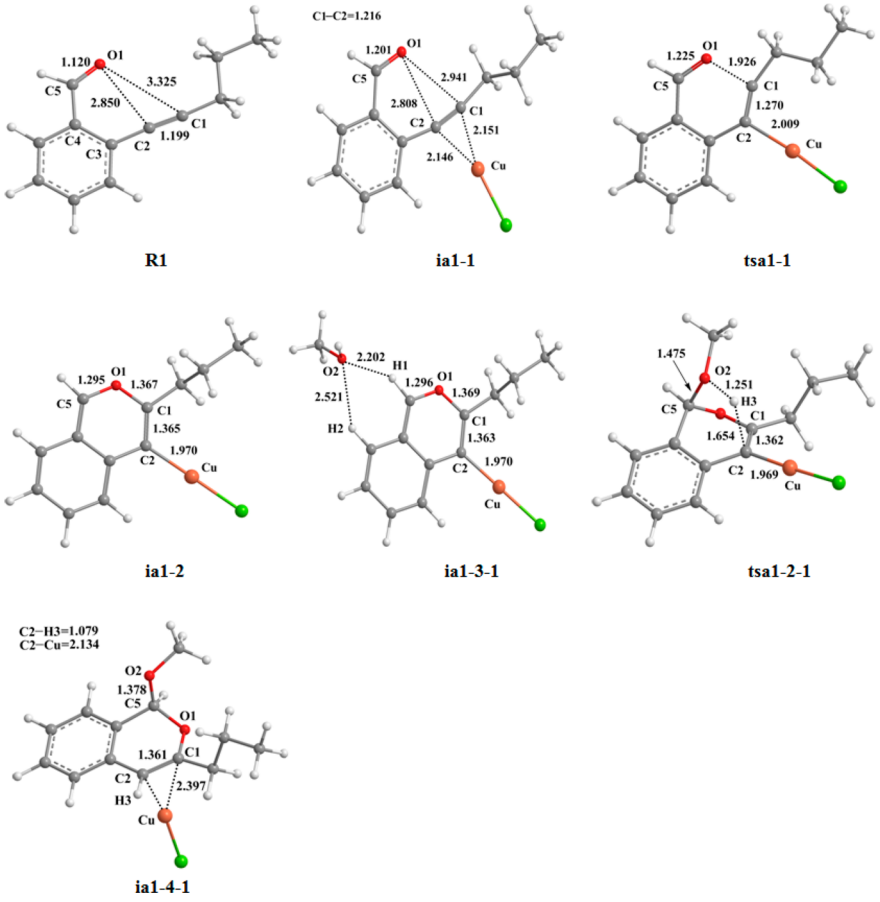

Figure 2. Optimized structures for the Cu(I)-catalyzed 6-endo model reaction without a cocatalyst in DMF medium [selected structural parameters are listed (bond lengths in angstroms)].

311++G** (Lanl2DZ for Cu) level. Unless specified, the discussed energies are the relative Gibbs free energies (ΔG_{sol}) in DMF solvent.

3. RESULTS AND DISCUSSION

3.1. Function of Solvent DMF. In this section, we first present the computational studies of the mechanisms of Cu(I)-catalyzed synthesis of cyclic alkenyl ethers with *o*-alkynylbenzaldehydes and MeOH in DMF medium, and then a detailed discussion of the solvent-assisted hydrogen shift process is presented to enhance our understanding of the role of DMF in the rate acceleration of this reaction.

3.1.1. Mechanism of Synthesis of Cyclic Alkenyl Ethers in DMF Medium. The DFT-computed energy surface of the 6-endo model reaction catalyzed by CuCl in DMF solvent is given in Figure 1, and the corresponding geometries along the reaction pathway are collected in Figure 2. The reaction begins with coordination of Cu(I) to the C≡C bond of substrate R1 (the structure of R1 is described in Figure 2). In principle, there are three kinds of models for the coordination of Cu(I) with R1, Cu(I)/O1, Cu(I)/(C1≡C2 and O1), and Cu(I)/C1≡C2. Unfortunately, the coordination mode of Cu(I)/O1 cannot be obtained by the various attempts in our calculations. For the second coordination mode, Cu(I)/(C1≡C2 and O1), it produces a complex ia1-1′, which is described in Figure S4 of the Supporting Information. It is clear that the carbonyl group (C5═O1) can be activated by Cu(I) in ia1-1′ to increase the eletrophilicity of C5, meaning that this coordination mode seems to be advantageous for the formation of hemiacetal via the intermolecular addition reaction of methanol and the carbonyl group of ia1-1′. In fact, the calculation results show that the hemiacetal cannot be formed because its formation needs to overcome the high energy barriers; the detailed mechanisms and the corresponding geometric structures along the reaction path are collected in Figures S1−S4 of the Supporting Information. In addition, the structure of ia1-1′ also shows that the coordination mode of Cu(I)/(C1≡C2 and O1) is dead-end for the intramolecular nucleophilic cyclization of O1 and the C1≡C2 bond. According to our calculations, one feasible strategy is to form the resonance-stabilized oxonium ion ia1-2 by the nucleophilic attack of aldehydic oxygen on the copper-coordinated alkynes (from ia1-1 to ia1-2 though tsa1-1, as shown in Figure 1), which would be trapped by the alcohol to form the final product P1. This mechanism has already been reported by Yamamoto, Abbiati, and Belmont.[9,18,30] In summary, the coordination of Cu(I) with C1≡C2 is the most favorable for the synthesis of cyclic alkenyl ethers. Besides, it is worth noting that the synthetic reaction was conducted under nonadiabatic conditions.[18] Although the formation of intermediates ia1-1 and ia1-1′ is very exothermic, the energies generated from the coordination process would be quickly released into the environment if the sample were being stirred and could not contribute to the following procedure. This similar fact has been supported by Zhang's group.[31] Therefore, the reactants need to be heated at 70 °C for 8 h to produce the final product P1.

As indicated by the calculation, the formation of complex ia1-1 is exergonic by 83.7 kJ/mol in DMF solvent. In ia1-1, the Cu−C1 and Cu−C2 bond lengths are 2.151 and 2.146 Å,

DOI: 10.1021/acs.joc.5b00523
J. Org. Chem. 2015, 80, 6553−6563

respectively. The bond length of the C1≡C2 bond increases to 1.216 Å, while the C5═O1 bond is extended to 1.201 Å. In addition, the APT charges of C1 and C2 are increased from +0.026 to +0.071 and from −0.307 to −0.103, respectively, while the APT charge of O1 is slightly decreased from −0.672 to −0.680. The changes in bond lengths and APT charges show that the coordination Cu(I)/C1≡C2 enhances the electrophilicity of the C1≡C2 bond and the nucleophilicity of the carbonyl O1, which can induce the following intramolecular cyclization.

The carbonyl oxygen O1 (as nucleophile) attacks the activated C1≡C2 bond to form an intermediate ia1-2 via a transition state tsa1-1 with a free energy barrier of 50.6 kJ/mol in DMF solvent (see Figure 1). In tsa1-1, the C1−O1 bond length is shortened from 2.941 Å (in ia1-1) to 1.926 Å, demonstrating that the C1−O1 bond is partly formed. In ia1-2, the C1−C2 bond completely changes from a triple bond to a double bond [$d_{(C1-C2)}$ of 1.365 Å] and the C1−O1 bond is completely formed [$d_{(C1-O1)}$ of 1.367 Å]. The C5−O1 bond also has some double-bond character, and the length is now 1.295 Å in ia1-2. Furthermore, the APT charges of C1, O1, and C5 are +0.409, −0.330, and +0.323, respectively. Both the structures mentioned above and the APT charges indicate that ia1-2 is an oxonium ion. The electrophilic property of the carbocation ($C5^+$) makes it easy to attack the nucleophile (MeOH) in a subsequent hydrogen-transfer reaction in ia1-2. Our calculations show that H3 of methanol can directly transfer to C2 to complete the catalytic cycle. In the H3-transfer process, ia1-2 first captures a MeOH with two hydrogen bonds, O2···H1−C [$d_{(O2-H1)}$ = 2.202 Å] and O2···H2−C [$d_{(O2-H2)}$ = 2.521 Å], to form a complex ia1-3-1, as described in Figure 2. The corresponding stabilization energy of ia1-3-1 is 11.2 kJ/mol relative to ia1-2 in DMF, indicating that the formation of ia1-3-1 is favorable in energy. A subsequent step generates an intermediate ia1-4-1 through O2 of MeOH (as nucleophile) attacking C5 (as an electrophile). This process requires an activation free energy barrier of 167.0 kJ/mol in DMF solvent via a transition state tsa1-2-1. In tsa1-2-1, the C5−O2, O2−H3, and H3−C2 bond lengths are 1.475, 1.251, and 1.654 Å, respectively. It is clear that the C5−O2 and H3−C2 bonds are partly formed while the O2−H3 bond is partly broken. These changes in bond distance show that the intermolecular nucleophilic addition and the hydrogen transfer occur at the same time, demonstrating that this is a concerted reaction. Finally, ia1-4-1 releases the product P1 and regenerates the catalyst CuCl. In principle, ia1-4-1 also can be formed through a stepwise addition reaction. We tried our best to find this stepwise addition but failed.

Figure 2 shows that the H3-transfer process, including the intermolecular nucleophilic addition, is the rate-limiting step of the whole reaction catalyzed by CuCl with a free energy barrier of 167.0 kJ/mol. Obviously, this barrier is too high to run this reaction. Thus, this direct H-shift mechanism is unfavorable for synthesis of the expected product in DMF solvent.

3.1.2. How Does Solvent DMF Promote the Reaction? Our calculations indicate that the synthesis of cyclic alkenyl ethers catalyzed by the Cu(I) complex is quite difficult on the basis of the direct H-shift mechanism because of the high free energy barrier (167.0 kJ/mol). In this section, we focus on how the DMF molecules promote the reaction rate of the tandem reaction. Theoretically, the DMF molecules can affect all steps of the entire reaction. In the intramolecular cyclization step, the DMF molecule coordinates with Cu(I) as a ligand, but this coordination does not alter the reaction mechanism of the intramolecular cyclization reaction, as shown in Scheme 2. The

Scheme 2. Comparison of the Activation Free Energies for the 6-Endo Cyclization Process without and with DMF in DMF Medium (DMF as a ligand)

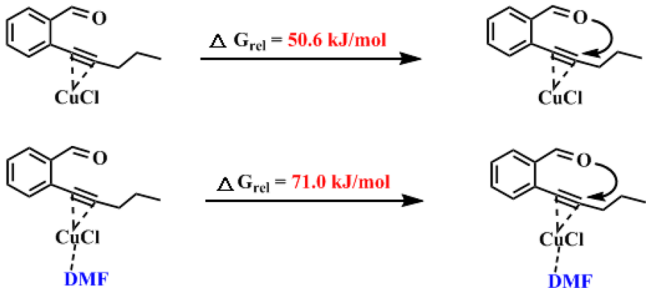

calculated activation free energy of the cyclization is 71.0 kJ/mol in the presence of DMF (as ligand), which is 20.4 kJ/mol higher than that in the case without the DMF as the ligand (50.6 kJ/mol). It is clear that the effect of DMF on the intramolecular cyclization process is negative. However, calculations indicate that the participation of DMF changes the direct hydrogen shift (involving the addition of the methanol hydroxyl oxygen and methanol hydroxyl hydrogen transfer) into a stepwise hydrogen-transfer process, which is quite similar to the proton-transfer processes in proton-transport catalysis[32] and many enzyme-catalyzed reactions.[33] More importantly, the present DMF-assisted hydrogen-transfer process can well explain the experimental phenomena.

In solution, our calculations show that the DMF molecule with Lewis base properties obtains a proton from substrate MeOH as an assisted catalyst[34] to facilitate the nucleophilic addition of methanol hydroxyl O2 with C5 and promote the transfer of H3 from O2 to C2. The energy profile for this process is shown in Figure 3, and the corresponding geometries are collected in Figure 4.

As illustrated in Figure 4, ia1-2 captures a MeOH molecule and a DMF molecule to generate an intermediate ia1-3-2. This process is exothermic by 37.5 kJ/mol relative to that of ia1-2. ia1-3-2 is stabilized by two kinds of interactions. One is a weak interaction between C5 and O2; the other is a O2−H3···O3 hydrogen bond, which is formed between the O2−H3 bond of MeOH and O3 of DMF. The C5···O2 and H3···O3 bond lengths in ia1-3-2 are 3.030 and 1.820 Å, respectively. The interaction between H3 and O2 is weakened because of the presence of the O2−H3···O3 hydrogen bond, which leads to the occurrence of intermolecular nucleophilic addition between O2 and C5 atoms. This case is more favorable than that in the direct H-transfer process (see Figures 1 and 3).

The following steps are DMF-mediated two-step proton-transfer processes, including a protonation of DMF (involved in the intermolecular nucleophilic addition reaction between C5 and O2) and a deprotonation of DMF-H^+. In the protonation of DMF, H3 connected with O2 is transferred to O3 of DMF. Concurrently, the intermolecular addition reaction between C5 and O2 also occurs. The net result of this process is generation of an intermediate ia1-4-2 via a transition state tsa1-2-2. In this step, the bond between O2 and H3 (1.557 Å in ia1-4-2) is broken and the C5−O2 and H3−O3 bonds (1.438 and 1.009 Å, respectively, in ia1-4-2) are formed. The breakage and formation of these bonds lead to a new O2···H3−O3

DOI: 10.1021/acs.joc.5b00523
J. Org. Chem. 2015, 80, 6553−6563

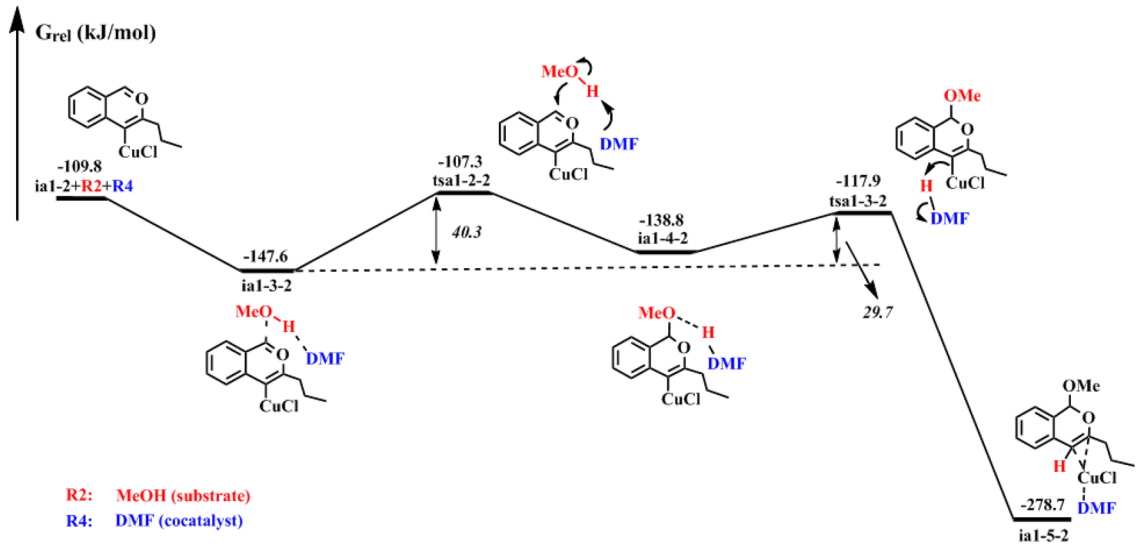

Figure 3. DFT-computed energy profile of the stepwise hydrogen-transfer process in the Cu(I)-catalyzed 6-endo model reaction with DMF as an assisted catalyst in DMF medium.

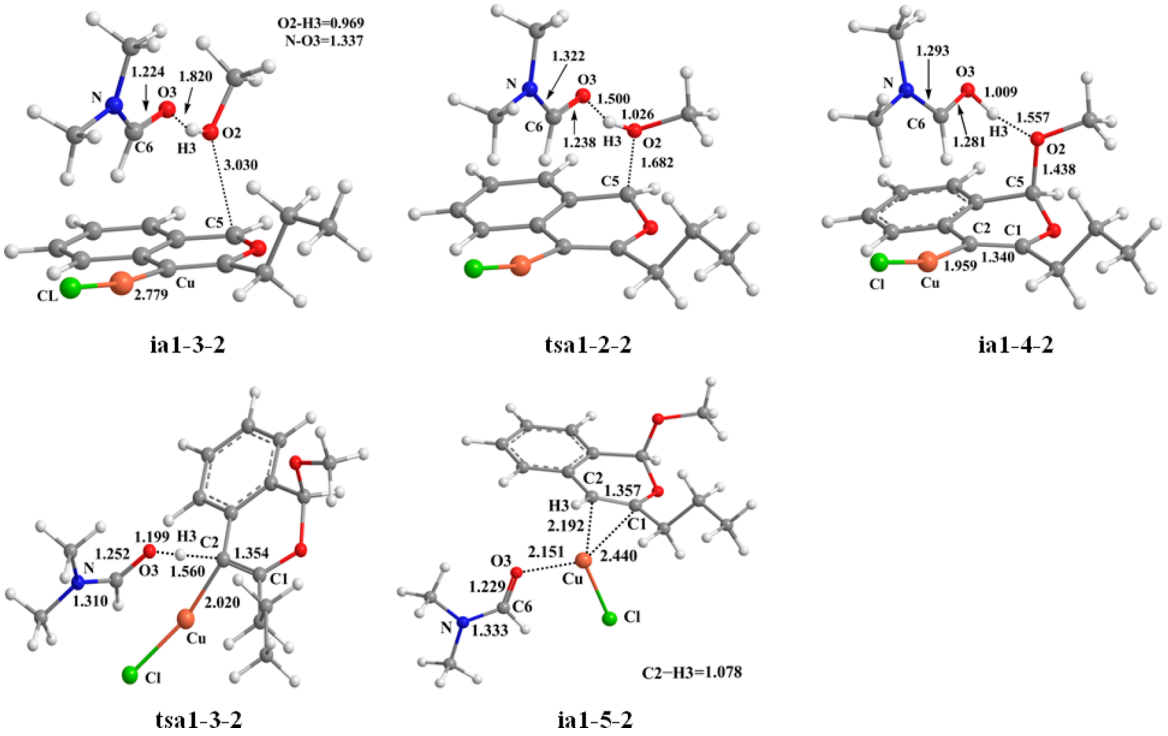

Figure 4. Optimized structures of the stepwise hydrogen-transfer process in the Cu(I)-catalyzed 6-endo model reaction with DMF as an assisted catalyst in DMF medium [selected structural parameters are listed (bond lengths in angstroms)].

hydrogen bond in ia1-4-2. In the transformation from ia1-3-2 to ia1-4-2, DMF acts as an electrophile to gain a proton from MeOH. The strategy used in this protonation is proton-transport catalysis, which is very similar to that adopted in some enzymatic reactions[33] involving general acid/base catalysis.

After uncovering the origin of protonation of DMF, next we turn our attention to explaining the reaction mechanism of deprotonation of DMF-H$^+$. In the deprotonation of DMF-H$^+$, ia1-4-2 transforms into ia1-5-2 via migration of a proton (H3) from protonated DMF (DMF-H$^+$) to C2 that is directly connected by CuCl. This reaction goes through a transition state tsa1-3-2. It is notable that the geometry of tsa1-3-2 is obtained through a loose scan from ia1-4-2 to ia1-5-2 along the formation of the H3−C2 bond, as illustrated in Figure 5. This method applied to search the transition state has been adopted successfully in the previous theoretical calculations.[35] In tsa1-3-2, the protonated DMF (as a proton donor) transfers a proton to C2 to produce a complex ia1-5-2 that will decompose into 6-endo product P1 and regenerate DMF and catalyst CuCl. In summary, in the two-step hydrogen-transfer strategy, solvent DMF plays a role as a proton shuttle to assist the transfer of H3 from MeOH to C2 of reactant R1. It should be emphasized that we tried our best to find two transition states and one additional intermediate in the transformation of ia1-4-2 to ia1-

DOI: 10.1021/acs.joc.5b00523
J. Org. Chem. 2015, 80, 6553−6563

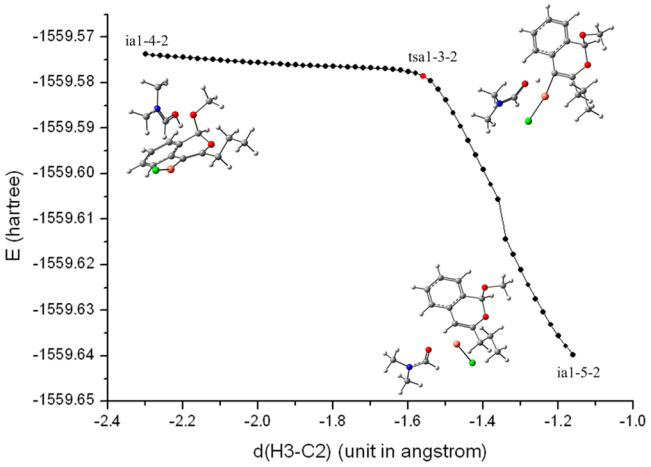

Figure 5. Loose scan profile from ia1-4-2 to ia1-5-2 along the formation of the H3−C1 bond in DMF medium (from 2.300 to 1.280 Å).

5-2 in which the protonated DMF and the CuCl complex are separated entities but failed.

Calculation results indicate that the present proton-transport catalytic strategy, involving the protonation of DMF and the deprotonation of DMF-H$^+$, is easy to implement in DMF solvent because of their lower free energy barriers (40.3 and 29.7 kJ/mol) compared with that of the direct H-shift process (Figure 1 vs Figure 3). This means that DMF can act as a proton shuttle to significantly reduce the free energy barriers of the proton-transport process. Furthermore, the rate-determining step is changed from the hydrogen shift process to the intermolecular cyclization step because of the participation of DMF. In the DMF-assisted catalytic mechanism, the free energy barrier of the rate-limiting step is 50.6 kJ/mol (see Figures 1 and 3), which is far lower than that of the direct hydrogen-transfer mechanism (167.0 kJ/mol).

The analysis described above shows that solvent DMF, which acts as a proton shuttle to lower the free energy barrier of the rate-limiting step, is critical in the stepwise proton-transport process. In addition, we are surprised to find that the substrate R2 (MeOH) can also play a similar role in the H-transport catalysis strategy because of its Lewis base character. This means that a transition metal-catalyzed reaction involving a similar hydrogen shift step can be accelerated when the solvent used is a Lewis base.

To explore the role of excessive MeOH in the CuCl-catalyzed reaction,[35,36] we substitute DMF with MeOH in the hydrogen-transfer mechanism. The calculated energy profile for this pathway is shown in Figure 6, and the geometries of involved intermediates and transition states are collected in Figure 7. The MeOH-assisted reaction is triggered by a weak interaction between ia1-2 and MeOH, leading to the production of a complex ia1-3-3. This process is exothermic by 25.3 kJ/mol with respect to that of ia1-2. Similar to the DMF catalytic process, the subsequent steps are the MeOH-mediated two-step hydrogen-transfer process, including a protonation of MeOH and a deprotonation of MeOH-H$^+$. In the protonation of MeOH, ia1-3-3 isomerizes to a new intermediate ia1-3-4 via a transition state tsa1-2-3. In tsa1-2-3, a MeOH molecule acts as a nucleophile to attack C5. Simultaneously, another MeOH molecule acting as a proton acceptor captures a proton from the nucleophile mentioned above to form a protonated MeOH (MeOH-H$^+$). In the deprotonation of MeOH-H$^+$, a proton of MeOH-H$^+$ is transferred to C2 that is directly connected by catalyst CuCl, via a transition state tsa1-3-3 to form a complex ia1-5-3. At last, the complex ia1-5-3 releases the 6-endo product P1, MeOH (as an assisted catalyst), and regenerates the catalyst CuCl to complete the catalytic reaction.

In the MeOH-assisted catalytic strategy, one of the MeOH molecules is used as a reactant and the other acts as a proton shuttle. Comparing Figures 3 and 6, we find that the mechanism of MeOH-assisted catalysis is similar to that of the DMF-assisted reaction. However, the rate-limiting step is changed from the intramolecular cyclization between O1 and C1 to the protonation of MeOH. Calculations indicate that the rate-determining step free energy barrier of the MeOH-assisted reaction (63.9 kJ/mol) is higher than that of the DMF-assisted

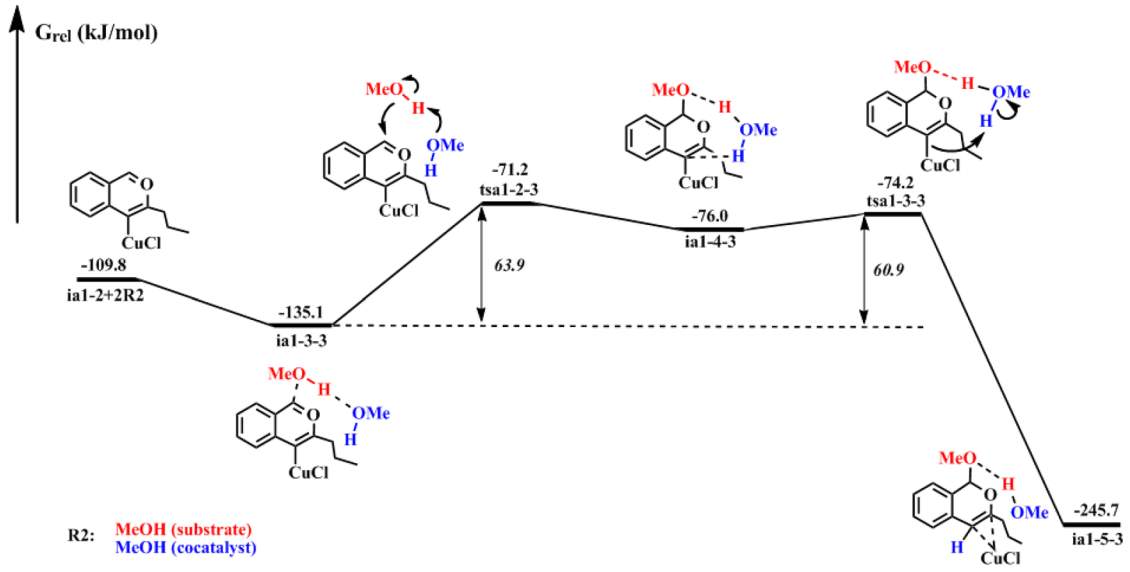

Figure 6. DFT-computed energy profile of the stepwise hydrogen-transfer process in the Cu(I)-catalyzed 6-endo model reaction with MeOH as an assisted catalyst in DMF medium.

DOI: 10.1021/acs.joc.5b00523
J. Org. Chem. 2015, 80, 6553−6563

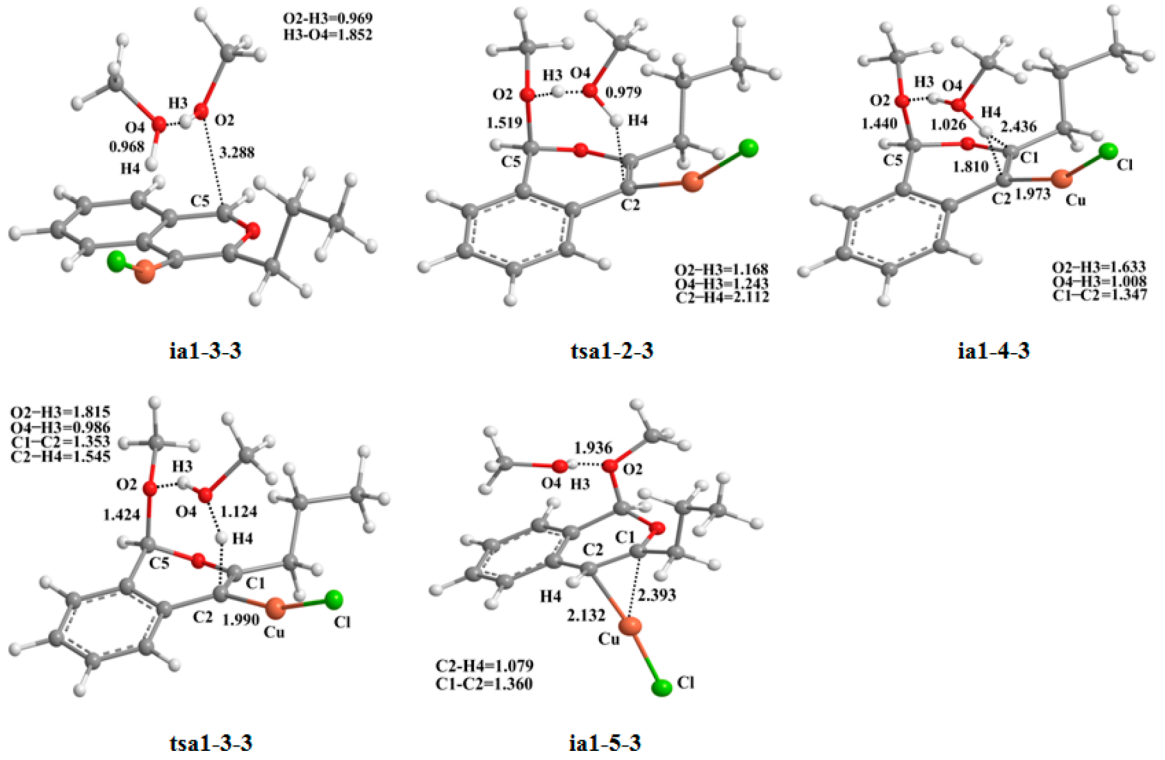

Figure 7. Optimized structures of the stepwise hydrogen-transfer process in the Cu(I)-catalyzed 6-endo model reaction with MeOH as an assisted catalyst in DMF medium [selected structural parameters are listed (bond lengths in angstroms)].

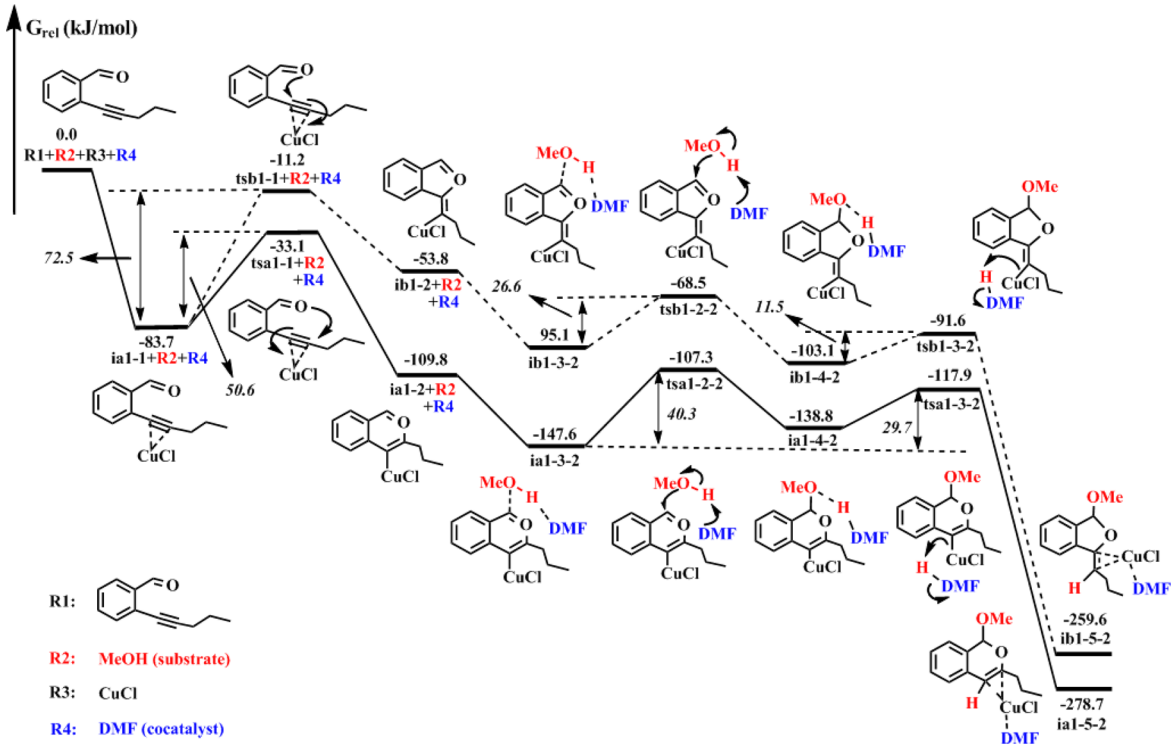

Figure 8. Optimal energy profiles for the Cu(I)-catalyzed reactions with DMF as an assisted catalyst in DMF medium.

reaction (50.6 kJ/mol), indicating that the former is inherently disfavored compared with the latter.

3.2. Influence of the Metallic Valence of Copper on Selectivity. Yamamoto and his co-workers found that the 6-endo product P1 is formed exclusively when Cu(I) salts (such as CuCl, CuBr, and CuI) are employed as catalysts, but the use of Cu(II) salt ($CuCl_2$) leads to a mixture of 5-exo P2 and 6-endo P1 in a 1:1 ratio.[18] These experimental results show that in DMF medium, the Cu(I) catalyst, but not the Cu(II) complex, has an excellent selectivity in the synthesis of cyclic alkenyl ethers via intramolecular cyclization of *o*-alkynylbenzaldehydes. However, we wonder how the metallic valence of

DOI: 10.1021/acs.joc.5b00523
J. Org. Chem. 2015, 80, 6553−6563

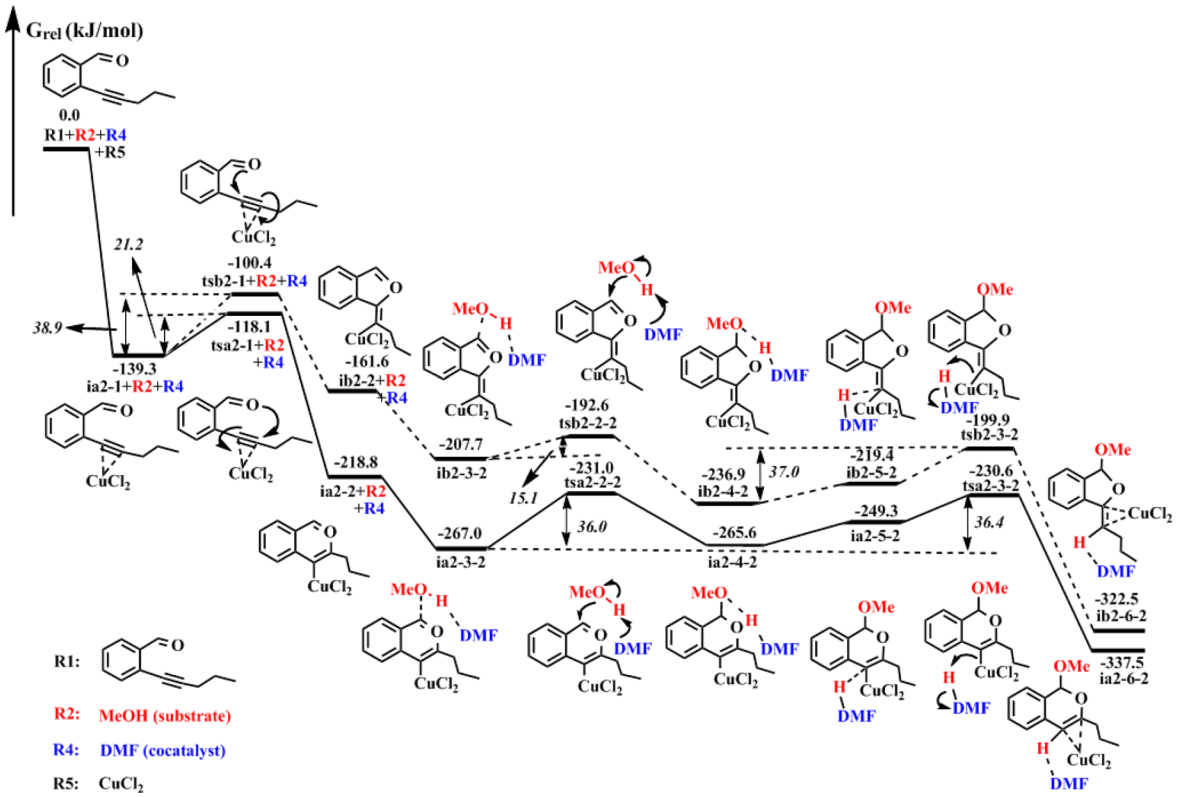

Figure 9. Optimal energy profiles for the Cu(II)-catalyzed reactions with DMF as an assisted catalyst in DMF medium.

copper [Cu(I) and Cu(II)] affects the selectivity. Generally, the details of reaction mechanisms cannot be easily accessed by experiments. Therefore, we present our theoretical studies of the Cu(I)- and Cu(II)-catalyzed synthesis of cyclic alkenyl ethers in DMF solvent, aiming to explore the reasons leading to different selectivities of Cu(I) and Cu(II) salts.

Our calculations show that the Cu(I)-catalyzed synthesis of 6-endo product P1 is favorable in energy, because of a low rate-determining free energy barrier (50.6 kJ/mol in DMF). The 5-exo model reaction, which is similar to the 6-endo one, also includes an intramolecular 5-exo cyclization and a stepwise hydrogen-transfer process (see Figure 8). The calculated free energy barriers of these processes are 72.5, 26.6, and 11.5 kJ/mol, respectively (the geometries of involved intermediates and transition states are collected in Figures S19 and S21 of the Supporting Information). Clearly, the cyclization reaction is also the rate-determining step for the 5-exo model reaction, and its free energy barrier (72.5 kJ/mol) is much higher than that of the 6-endo model (50.6 kJ/mol). This means that the 6-endo product P1 can be exclusively obtained when Cu(I) salt is used as a metal catalyst. Actually, the cyclization is a nucleophilic addition reaction, in which carbonyl O1 of ia1-1 attacks C1 and C2. In ia1-1, the APT charges for C1 and C2 atoms are +0.071 and −0.103, respectively, indicating that the nucleophilic attack of O1 on C1 is easier than on C2. In addition, the APT charge for C1 is changed to +0.772 in tsa1-1, which is 0.585 higher than that for C2 (+0.187) in tsb1-1. The results related to the APT charges suggest that the Cu(I)-catalyzed reaction will lead to the formation of the O1−C1 bond and finally produce exclusively the 6-endo product P1.

Why was a mixture of 5-exo P2 and 6-endo P1 obtained in a 1:1 ratio when the Cu(II) catalyst was used in the experiments? Figure 9 displays the calculated energy profiles of $CuCl_2$-catalyzed reactions with DMF as an assisted catalyst (the geometries of intermediates and transition states are collected in Figures S25 and S27 of the Supporting Information). By comparing Figures 8 and 9, the CuCl- and $CuCl_2$-catalyzed reactions have a similar mechanism, including an intramolecular cyclization and a two-step hydrogen-transfer process. It is noteworthy that the rate-determining steps of the $CuCl_2$-catalyzed reactions are partly changed compared with those of the CuCl-catalyzed reactions because of the effect of different valence states of copper. The rate-determining step of the $CuCl_2$-catalyzed 5-exo model reaction is still the cyclization reaction with a required energy of 38.9 kJ/mol, but that of the $CuCl_2$-catalyzed 6-endo model reaction is changed into the deprotonation of DMF with a required energy of 36.4 kJ/mol (relative to the stable intermediate ia2-3-2). This difference in energy of 2.5 kJ/mol is quite small, which means that the 5-exo model and 6-endo model reactions catalyzed by $CuCl_2$ can be conducted at the same rate. Further, Figure 9 reveals that the formation of intermediate ia2-3-2 (ib2-3-2) from ia2-1 via transition structure tsa2-1 (tsb2-1) is an irreversible reaction because the next barriers are all lower than the reverse barrier of this step [from ia2-3-2 (ib2-3-2) to tsa2-1 (tsb2-1)], indicating that the determining steps of selectivity for the 6-endo and 5-exo models are tsa2-1 and tsb2-1, respectively. Evidently, the two barriers (21.2 vs 38.9 kJ/mol) are not equal, which shows that the results presented here do not seem to support the experimental finding that a mixture of 5-exo and 6-endo products was obtained in a 1:1 ratio.[18] However, under the experimental condition[18] (the reactants were heated at 70 °C for 8 h), the two low-energy barriers (21.2 and 38.9 kJ/mol) are easy to exceed; thus, the 5-exo and 6-endo products can be generated at the same time.

DOI: 10.1021/acs.joc.5b00523
J. Org. Chem. 2015, 80, 6553−6563

3.2.1. How To Understand the Selectivity Difference in Cu(I)- and Cu(II)-Catalyzed Reactions. In this section, the charge decomposition analysis (CDA) and the constructed orbital interaction diagrams are used to explore this interesting issue. Complexes ia1-1 and ia2-1 are chosen as a studied system because the selectivity depends on their electronic structures. The electronic interactions between substrate R1 (fragment 1) and catalyst (CuCl or $CuCl_2$, fragment 2) are calculated by the AOMix-CDA program [on the basis of the BhandHLYP/6-31G* results, α and β denote the α and β molecular orbitals (MOs), respectively, of ia2-1], and the orbital interaction diagrams are shown in Figures 10 and 11. For the CuCl-catalyzed reaction, the calculated electrons results show that the occupied molecular orbital HOMO-8 of ia1-1 is related to the C1−Cu and C2−Cu coordination bonds. According to the results of the molecular orbital fragment analyses, HOMO-8 of ia1-1 is composed of 1.2% HOFO-3 (the HOMO-3 of fragment orbitals) of R1 and 4.4% HOFO-3, 89.7% HOFO-4, and 1.8% HOFO-7 of fragment 2 (CuCl). It is clear that the composition of HOMO-8 is mainly from catalyst CuCl. More importantly, the net charge donation, including both charge donation and electronic polarization contributions, is only 0.243 electrons from fragment 1 to fragment 2. Similarly, for the $CuCl_2$-catalyzed reaction, HOMO-9 of ia2-1 is related to the C1−Cu and C2−Cu coordination bonds. In contrast with the CuCl-catalyzed case, the contribution of HOMO-9 is mainly from substrate R1. Further, the net charge donation (including the net charge donation of 0.123 electrons for α MOs and the charge donation of 0.256 electrons for β MOs) is beyond 0.379 electrons from fragment 1 to fragment 2. On the basis of the analysis described above for ia1-1 and ia2-1, these results reveal that the coordination capability of Cu(II) with R1 is much stronger than that of Cu(I) with R1 (0.243 electrons in ia1-1 vs 0.379 electrons in ia2-1 for the net charge donation from fragment 1 to fragment 2), which is just the reason that the intramolecular cyclization has lower activation energies in the $CuCl_2$-catalyzed reactions. In a word, because of the stronger coordination capability, the Cu(II) salts can greatly decrease the cyclization free energy barriers of the 5-exo and 6-endo model reactions. This partly changes the rate-determining steps of the $CuCl_2$-catalyzed reactions as compared to that of CuCl-catalyzed reactions and finally results in the different selectivity of CuCl and $CuCl_2$ in DMF medium. A similar explanation can also be obtained from the orbital interaction diagram of tsa1-1 versus tsa2-1 and tsb1-1 versus tsb2-1 (shown in Figures S30−S33 of the Supporting Information). This fact can also be confirmed by comparing the stabilization energies of ia1-1 and ia2-1 (83.7 vs 139.3 kJ/mol), as indicated in Figures 8 and 9. Of course, this conclusion needs to be proven in future work.

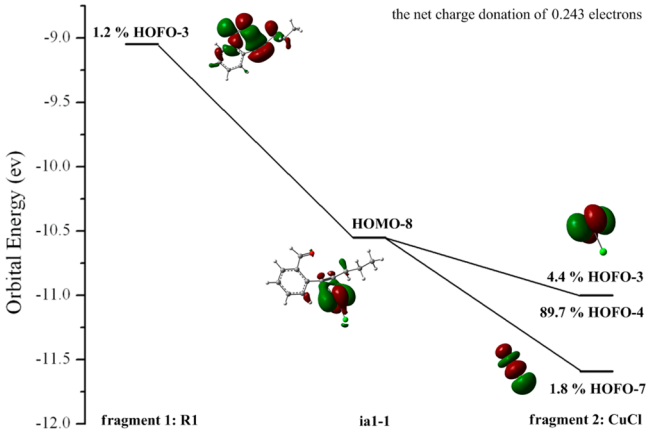

Figure 10. Orbital interaction diagram illustrating the coupling of the R1 and CuCl fragments in the ia1-1 complex (the AOMix-CDA calculation at the BhandHLYP/6-31G* level; the net charge donation is 0.243 electrons from fragment 1 to fragment 2).

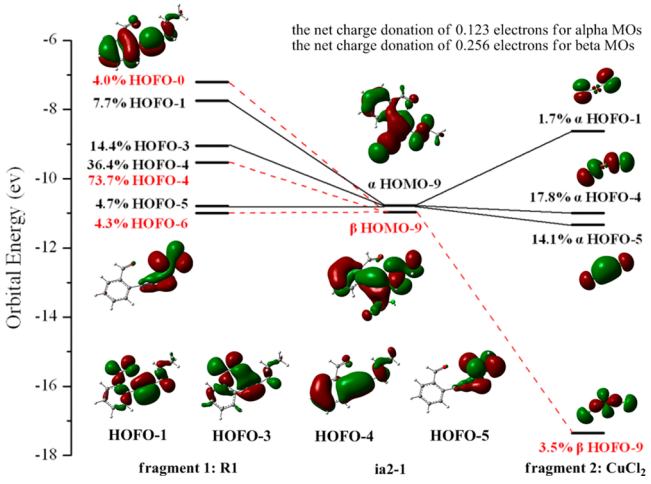

Figure 11. α,β-Spin orbital interaction diagram illustrating the coupling of the R1 and $CuCl_2$ fragments in the ia2-1 complex (the AOMix-CDA calculation at the BhandHLYP/6-31G* level; α and β MOs are colored black and red, respectively; the net charge donation, including the net charge donation of 0.123 electrons for α MOs and the charge donation of 0.256 electrons for β MOs, is 0.379 electrons from fragment 1 to fragment 2).

3.3. Roles of CuCl and $CuCl_2$ in the Present Cu(I)- and Cu(II)-Catalyzed Cyclization. The calculation results presented above rationalize the experimental observations[18] when catalysts CuCl and $CuCl_2$ take part in the cyclization of *o*-alkynylbenzaldehydes. In this section, we focus on whether the cyclization will occur without CuCl and $CuCl_2$. To illuminate the effect of CuCl and $CuCl_2$ on the reaction, the mechanisms of the cyclization of *o*-alkynylbenzaldehydes without metal catalysts are studied. The calculated energy profiles of the 5-exo and 6-endo cyclization processes are shown in Figure 12, and the corresponding geometries are collected in Figure S34 of the Supporting Information. Starting from substrate R1, the reaction forms the intermediates ib3-2 and ia3-2 via the 5-exo and 6-endo cyclization with transformation required energies of

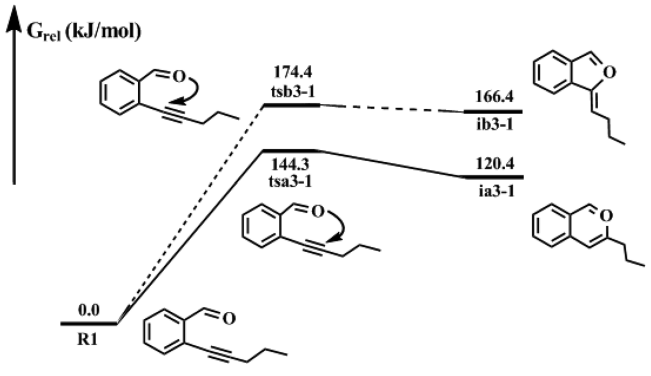

Figure 12. DFT-computed energy profiles for the 5-exo and 6-endo cyclization reactions without a metal catalyst in DMF medium.

DOI: 10.1021/acs.joc.5b00523
J. Org. Chem. 2015, 80, 6553−6563

174.4 and 144.3 kJ/mol, respectively. Obviously, the cyclization reaction cannot occur in the absence of metal catalyst CuCl or $CuCl_2$, indicating metal catalysts CuCl and $CuCl_2$ are prerequisites for the producion of the cyclic alkenyl ethers via an intramolecular cyclization of *o*-alkynylbenzaldehydes.

4. CONCLUSIONS

Here, the mechanisms of the Cu(I)- and Cu(II)-catalyzed cyclization of *o*-alkynylbenzaldehydes are computationally addressed using the DFT method (BhandHLYP/6-31G*, LanL2DZ for the Cu atom). Calculation results indicate that Cu(I) catalysts are effective for the synthesis of cyclic alkenyl ethers. Importantly, the important role of solvent DMF is revealed; it can promote the stepwise hydrogen-transfer process, including the protonation of DMF and deprotonation of DMF-H^+. In the whole proton migration process, DMF acts as a proton shuttle to assist a proton migration from MeOH to the carbon atom. In addition, we find that the substrate MeOH also plays a role similar to that of DMF in the proton-transport catalytic strategy, whereas its catalytic capability is weaker than that of the DMF. It is worth mentioning that the appropriate metallic valence of copper is crucial for the selective synthesis of the target product. In this work, the Cu(I) salts are selected as effective metal catalysts to exclusively produce the 6-endo product P1. Calculations also reveal that a transition metal-catalyzed reaction involving a hydrogen shift step can be accelerated when the solvent used has Lewis base natures. These findings and insights should be valuable for the understanding of the Cu(I)- and Cu(II)-catalyzed synthesis of cyclic alkenyl ethers from *o*-alkynylbenzaldehydes with MeOH (in DMF solution) and be expected to help us design other new reactions.

■ ASSOCIATED CONTENT

Supporting Information

DFT-computed energy profiles of all potential reaction pathways, optimized geometries of all involved species, intrinsic reaction coordinates of some key transition states, etc. The Supporting Information is available free of charge on the ACS Publications website at DOI: 10.1021/acs.joc.5b00523.

■ AUTHOR INFORMATION

Corresponding Author

*E-mail: liming@swu.edu.cn.

Notes

The authors declare no competing financial interest.

■ ACKNOWLEDGMENTS

We acknowledge generous financial support from the Fundamental Research Funds for the Central Universities (Grant XDJK2013A008). R.X.H. acknowledges the financial support from the Natural Science Foundation of China (21173169) and the Fundamental Research Funds for the Central Universities (No. XDJK2013A008).

■ REFERENCES

(1) (a) Chen, D. G.; Xu, C.; Deng, J.; Jiang, C. H.; Wen, X. A.; Kong, L. Y.; Zhang, J.; Sun, H. B. *Tetrahedron* **2014**, *70*, 1975−1983. (b) Kobayashi, K.; Kondo, Y. *Org. Lett.* **2009**, *11* (9), 2035−2037. (c) Ruiz-Pernía, J. J.; Martí, S.; Moliner, V.; Tuñón, I. *J. Chem. Theory Comput.* **2012**, *8*, 1532−1535. (d) Krauter, C. M.; Hashmi, A. S. K.; Pernpointner, M. *ChemCatChem* **2010**, *2*, 1226−1230. (e) Solà, M.; Lledós, A.; Duran, M.; Bertrán, J.; Abboud, J. B. M. *J. Am. Chem. Soc.* **1991**, *113*, 2873−2879. (f) Smallwood, I. *Handbook of Organic Solvent Properties*; Butterworth-Heinemann: New York, 1989. (g) Reichardt, C.; Welton, T. *Solvents and Solvent Effects in Organic Chemistry*; John Wiley & Sons: New York, 2011.

(2) (a) Cai, C.; Chung, J. Y. L.; McWilliams, J. C.; Sun, Y.; Shultz, C. S.; Palucki, M. *Org. Process Res. Dev.* **2007**, *11*, 328−335. (b) Lee, S.-S.; Kim, H.-S.; Hwang, T.-K.; Oh, Y.-H.; Park, S.-W.; Lee, S. *Org. Lett.* **2008**, *10* (1), 61−64. (c) Dubbaka, S. R.; Narreddula, V. R.; Gadde, S.; Mathew, T. *Tetrahedron* **2014**, *70*, 9676−9681. (d) Colombo, T. S.; Mazutti, M. A.; Di Luccio, M.; de Oliveira, D.; Oliveira, J. V. *J. Supercrit. Fluids* **2015**, *97*, 16−21. (e) Guan, Z.; Song, J.; Xue, Y.; Yang, D.-C.; He, Y.-H. *J. Mol. Catal. B: Enzym.* **2015**, *111*, 16−20. (f) Liese, A.; Hilterhaus, L. *Chem. Soc. Rev.* **2013**, *42* (15), 6236−6249. (g) Shafiei, M.; Ziaee, A.-A.; Amoozegar, M. A. *J. Ind. Microbiol. Biotechnol.* **2011**, *38* (2), 275−281. (h) Zhou, Z.; Hartmann, M. *Chem. Soc. Rev.* **2013**, *42* (9), 3894−3912. (i) Scheerle, R. K.; Grassmann, J.; Letzel, T. *Anal. Sci.* **2012**, *28* (6), 607−612.

(3) (a) Belting, V.; Krause, N. *Org. Biomol. Chem.* **2009**, *7*, 1221−1225. (b) Yan, W. M.; Wang, Q. Y.; Chen, Y. F.; Petersen, J. L.; Shi, X. D. *Org. Lett.* **2010**, *12* (15), 3308−3311. (c) Li, H.; Li, Y.; Zhang, X.-S.; Chen, K.; Wang, X.; Shi, Z.-J. *J. Am. Chem. Soc.* **2011**, *133* (39), 15244−15247. (d) Pieri, C.; Combes, S.; Brunel, J. M. *Tetrahedron* **2014**, *70*, 9718−9725.

(4) (a) Ding, S. T.; Jiao, N. *J. Am. Chem. Soc.* **2011**, *133*, 12374−12377. (b) Mazzone, G.; Russo, N.; Sicilia, E. *Organometallics* **2012**, *31*, 3074−3080. (c) Kendale, J. C.; Valentin, E. M.; Woerpel, K. *Org. Lett.* **2014**, *16* (14), 3684−3687.

(5) Choe, Y.; Lee, P. H. *Org. Lett.* **2009**, *11* (6), 1445−1448.

(6) (a) Chen, B.; Fan, W.; Chai, G. B.; Ma, S. M. *Org. Lett.* **2012**, *14* (14), 3616−3619. (b) He, C.; Guo, S.; Ke, J.; Hao, J.; Xu, H.; Chen, H. Y.; Lei, A. W. *J. Am. Chem. Soc.* **2012**, *134*, 5766−5769.

(7) (a) Do, H.-Q.; Daugulis, O. *J. Am. Chem. Soc.* **2008**, *130*, 1128−1129. (b) Shende, V. S.; Kuriakose, N.; Vanka, K.; Kelkar, A. A.; Shingote, S. K.; Deshpande, S. H. *RSC Adv.* **2014**, *4*, 46351−46356.

(8) Chen, Z. Y.; Yang, X. D.; Wu, J. *Chem. Commun.* **2009**, 3469−3471.

(9) Patil, N. T.; Wu, H.; Yamamoto, Y. *J. Org. Chem.* **2005**, *70*, 4531−4534.

(10) (a) Barange, D. K.; Nishad, T. C.; Swamy, N. K.; Bandameedi, V.; Kumar, D.; Sreekanth, B. R.; Vyas, S. K.; Pal, M. *J. Org. Chem.* **2007**, *72*, 8547−8550. (b) Sakata, K.; Fujimoto, H. *Organometallics* **2010**, *29*, 1004−1011. (c) Xia, Y. Z.; Huang, G. P. *J. Org. Chem.* **2010**, *75*, 7842−7854.

(11) Wang, X. C.; Weigl, C.; Doyle, M. P. *J. Am. Chem. Soc.* **2011**, *133*, 9572−9579.

(12) Peng, L. L.; Zhang, X.; Zhang, S. W.; Wang, J. B. *J. Org. Chem.* **2007**, *72*, 1192−1197.

(13) Sromek, A. W.; Rubina, M.; Gevorgyan, V. *J. Am. Chem. Soc.* **2005**, *127*, 10500−10501.

(14) (a) Anderson, J. R., Boudart, M., Eds. *Catalysis: Science and Technology*; Springer-Verlag: Berlin, 1984. (b) McQuillin, F. J.; Parker, D. G.; Stephenson, G. R. *Transition Metal Organometallics for Organic Synthesis*; Cambridge Press: New York, 1991.

(15) Fang, Y. W.; Li, C. Z. *Chem. Commun.* **2005**, 3574−3576.

(16) (a) Zhang, L.; Ye, D. J.; Zhou, Y.; Liu, G. N.; Feng, E. G.; Jiang, H. L.; Liu, H. *J. Org. Chem.* **2010**, *75*, 3671−3677. (b) Xia, Y. Z.; Dudnik, A. S.; Gevorgyan, V.; Li, Y. H. *J. Am. Chem. Soc.* **2008**, *130*, 6940−6941.

(17) Peng, L. L.; Zhang, X.; Zhang, S. W.; Wang, J. B. *J. Org. Chem.* **2007**, *72*, 1192−1197.

(18) Patil, N. T.; Yamamoto, Y. *J. Org. Chem.* **2004**, *69*, 5139−5142.

(19) Gilmore, K.; Alabugin, I. *Chem. Rev.* **2011**, *111*, 6513−6556.

(20) Frisch, M. J.; Trucks, G. W.; Schlegel, H. B.; Scuseria, G. E.; Robb, M. A.; Cheeseman, J. R.; Scalmani, G.; Barone, V.; Mennucci, B.; Petersson, G. A.; Nakatsuji, H.; Caricato, M.; Li, X.; Hratchian, H. P.; Izmaylov, A. F.; Bloino, J.; Zheng, G.; Sonnenberg, J. L.; Hada, M.; Ehara, M.; Toyota, K.; Fukuda, R.; Hasegawa, J.; Ishida, M.; Nakajima, T.; Honda, Y.; Kitao, O.; Nakai, H.; Vreven, T.; Montgomery, J. A., Jr.; Peralta, J. E.; Ogliaro, F.; Bearpark, M.; Heyd, J. J.; Brothers, E.; Kudin,

DOI: 10.1021/acs.joc.5b00523
J. Org. Chem. 2015, 80, 6553−6563

K. N.; Staroverov, V. N.; Kobayashi, R.; Normand, J.; Raghavachari, K.; Rendell, A.; Burant, J. C.; Iyengar, S. S.; Tomasi, J.; Cossi, M.; Rega, N.; Millam, J. M.; Klene, M.; Knox, J. E.; Cross, J. B.; Bakken, V.; Adamo, C.; Jaramillo, J.; Gomperts, R.; Stratmann, R. E.; Yazyev, O.; Austin, A. J.; Cammi, R.; Pomelli, C.; Ochterski, J. W.; Martin, R. L.; Morokuma, K.; Zakrzewski, V. G.; Voth, G. A.; Salvador, P.; Dannenberg, J. J.; Dapprich, S.; Daniels, A. D.; Farkas, O.; Foresman, J. B.; Ortiz, J. V.; Cioslowski, J.; Fox, D. J. *Gaussian 09*, revision A.02; Gaussian, Inc.: Wallingford, CT, 2009.

(21) Parr, R. G.; Yang, W. *Density-functional Theory of Atoms and Molecules*; Oxford University Press: New York, 1989.

(22) Becke, A. D. *J. Chem. Phys.* **1993**, *98*, 1372−1377.

(23) Lee, C.; Yang, W.; Parr, R. G. *Phys. Rev. B* **1988**, *37*, 785−789.

(24) (a) Zhang, Q.; Bell, R.; Truong, T. N. *J. Phys. Chem.* **1995**, *99*, 592−599. (b) Lynch, B. J.; Fast, P. L.; Harris, M.; Truhlar, D. G. *J. Phys. Chem. A* **2000**, *104*, 4811−4815. (c) Espinosa-García, J. *J. Am. Chem. Soc.* **2004**, *126*, 920−927. (d) Wille, U.; Tan, J. C.-S.; Mucke, E.-K. *J. Org. Chem.* **2008**, *73*, 5821−5830.

(25) (a) Hehre, W. J.; Ditchfield, R.; Pople, J. A. *J. Chem. Phys.* **1972**, *56*, 2257−2261. (b) Rassolov, V. A.; Pople, J. A.; Ratner, M. A.; Windus, T. L. *J. Chem. Phys.* **1998**, *109*, 1223−1229. (c) Rassolov, V. A.; Ratner, M. A.; Pople, J. A.; Redfern, P. C.; Curtiss, L. A. *J. Comput. Chem.* **2001**, *22*, 976−984.

(26) (a) Hay, P. J.; Wadt, W. R. *J. Chem. Phys.* **1985**, *82*, 270−283. (b) Wadt, W. R.; Hay, P. J. *J. Chem. Phys.* **1985**, *82*, 284−298. (c) Hay, P. J.; Wadt, W. R. *J. Chem. Phys.* **1985**, *82*, 299−310.

(27) Gonzalez, C.; Schlegel, H. B. *J. Phys. Chem.* **1990**, *94*, 5523−5527.

(28) (a) Gorelsky, S. I.; Lever, A. B. P. *J. Organomet. Chem.* **2001**, *635*, 187−196. (b) Gorelsky, S. I. *AOMix: Program for Molecular Orbital Analysis*; York University: Toronto (http://www.sg-chem.net).

(29) (a) Gonzalez, C.; Schlegel, H. B. *J. Chem. Phys.* **1989**, *90*, 2154−2161. (b) Tomasi, J.; Persico, M. *Chem. Rev.* **1994**, *94*, 2027−2094. (c) Mineva, T.; Russo, N.; Sicilia, E. *J. Comput. Chem.* **1998**, *19*, 290−299. (d) Cossi, M.; Scalmani, G.; Rega, N.; Barone, V. *J. Chem. Phys.* **2002**, *117*, 43−54.

(30) (a) Dell'Acqua, M.; Castano, B.; Cecchini, C.; Pedrazzini, T.; Pirovano, V.; Rossi, E.; Caselli, A.; Abbiati, G. *J. Org. Chem.* **2014**, *79*, 3494−3505. (b) Godet, T.; Vaxelaire, C.; Michel, C.; Milet, A.; Belmont, P. *Chem.—Eur. J.* **2007**, *13*, 5632−5641.

(31) Liu, Y. X.; Zhang, D. J.; Bi, S. W. *J. Phys. Chem. A* **2010**, *114*, 12893−12899.

(32) (a) Shi, F.-Q.; Li, X.; Xia, Y. Z.; Zhang, L. M.; Yu, Z.-X. *J. Am. Chem. Soc.* **2007**, *129*, 15503−15512. (b) Nakamura, I.; Shiraiwa, N.; Kanazawa, R.; Terada, M. *Org. Lett.* **2010**, *12* (18), 4198−4200. (c) Verma, P.; Patni, P. A.; Sunoj, P. B. *J. Org. Chem.* **2011**, *76*, 5606−5611. (d) Roy, D.; Patel, C.; Sunoj, R. B. *J. Org. Chem.* **2009**, *74*, 6936−6943. (e) Zhang, X.; Houk, K. N. *J. Org. Chem.* **2005**, *70*, 9712−9716.

(33) (a) For a thematic issue on the studies of enzymatic reaction mechanisms, see: Schramm, V. L. *Chem. Rev.* **2006**, *106*, 3029−3030 and references therein. (b) Gao, J.; Ma, S.; Major, D. T.; Nam, K.; Pu, J.; Truhlar, D. G. *Chem. Rev.* **2006**, *106*, 3188−3209. (c) Ragsdale, S. W. *Chem. Rev.* **2006**, *106*, 3317−3337. (d) Zhang, X.; Houk, K. N. *Acc. Chem. Res.* **2005**, *38*, 379−385. (e) Bruice, T.; Yurkanis, P.; Bruice, Y. *J. Am. Chem. Soc.* **2005**, *127*, 12478−12479.

(34) DMF can assist proton transfer. See: (a) Patil, N. T.; Wu, H.; Yamamota, Y. *J. Org. Chem.* **2005**, *70*, 4531−4534. (b) Sharma, A. K.; Sunoj, R. B. *Angew. Chem.* **2010**, *122*, 6517−6521.

(35) Zhang, J. S.; Shen, W.; Li, L. Q.; Li, M. *Organometallics* **2009**, *28*, 3129−3139.

(36) Kovács, G.; Lledós, A.; Ujaque, G. *Organometallics* **2010**, *29*, 3252−3260.

DOI: 10.1021/acs.joc.5b00523
J. Org. Chem. 2015, 80, 6553−6563